ACCEPTED MANUSCRIPT

Silicon Y-bifurcated microchannels etched in 25 wt % TMAH water solution

Silicon Y-bifurcated microchannels etched in 25 wt % TMAH water solution

Milče M. Smiljanić[1], Žarko Lazić[1], Milena Rašljić Rafajilović[1], Katarina Cvetanović Zobenica[1], Evgenija Milinković[1] and Ana Filipović[1]

[1]University of Belgrade-Institute of Chemistry, Technology and Metallurgy, National Institute of the Republic of Serbia ICTM, Department of Microelectronic Technologies, Serbia

E-mail: smilce@nanosys.ihtm.bg.ac.rs

Abstract

In this study, Y-bifurcated microchannels fabricated from a {100} silicon in 25 wt % TMAH water solution at the temperature of 80 °C have been presented and analysed. We studied the etching of acute angles with sides along the <n10> crystallographic directions in the masking layer where $1 < n < 8$. We considered symmetrical acute corners in the masking layer with respect to the <100> crystallographic directions. The angles between the appropriate <n10> and <100> crystallographic directions were smaller than 45 °. Moreover, we observed asymmetrical acute corners formed by the <n10> and <m10> crystallographic directions, where m≠n. We found that the obtained convex corners were not distorted during etching. Consequently, it is not necessary to apply convex corner compensation. These fabricated undistorted convex corners represent the angles of the bifurcations. The sidewalls of the microchannels are defined by etched planes of the {n11} and {100} families. Analytical relations were derived for the widths of the microchannels. The results enable simple and cost-effective fabrication of various complex silicon microfluidic platforms.

Keywords: Y bifurcation, microchannels, silicon, wet etching, TMAH

1. Introduction

Many studies have explored micromachining of (100) silicon substrates using anisotropic wet etching in 25 wt % tetramethylammonium hydroxide (TMAH) water solution [1-28]. The etch rates of crystallographic planes [1–13,15,26], roughness of silicon surface after etching [2,7,13,25], and problems of convex corner etching and their solutions [14–28] have been investigated. Pattern design in the masking layer and solution anisotropy determine the etched three-dimensional (3D) silicon shape. The distortion of convex corners during etching limits the production methods of complicated 3D silicon shapes [2,14,22,26]. The applied convex corner compensation depends on the design of the microdevice. Most of the designs are developed for the

patterns with sides along the <110> crystallographic directions [15–24]. Some of them cause unwanted residues at the bottom of the silicon structure at the end of etching [19,22]. These residues can influence the functioning of microdevices. Moreover, the sides of the pattern designs are only along the most common crystallographic directions <110> and <100>.

In our previous work [26–28], we presented a comprehensive study on the etching of patterns with sides along the <n10> crystallographic directions. In these papers, we presented etching of the (100) silicon in 25 wt % TMAH water solution at the temperature of 80 °C, using silicon dioxide as a masking layer. We explored the etching of mask patterns in the shapes of squares and parallelograms in the corresponding studies. In Ref.[26], we studied square islands

and apertures with sides along the <n10> crystallographic directions, where $0 \leq n < 10$. In [27–28], we analysed islands in the shapes of parallelograms with sides along predetermined crystallographic directions <n10> ($1 < n < 8$) and <100>. During the etching of patterns presented in Ref.[28], sustainable types of 3D silicon shapes were obtained. It was concluded that the convex corners were not distorted, although, no convex corner compensation was applied.
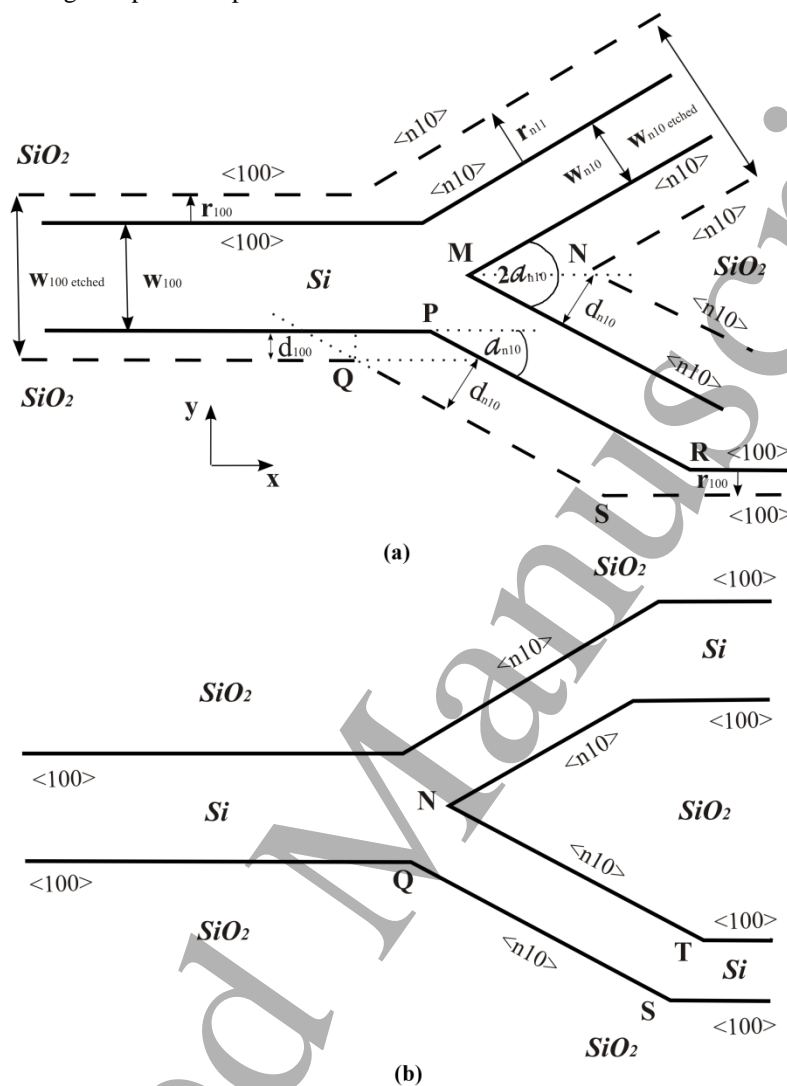

Figure 1. a) Schematic picture of Y-bifurcated microchannel's etching evolution. b) Schematic picture of two level microfluidic network.

This technical note presents our new results on the (100) silicon etching in 25 wt % TMAH water solution at a temperature of 80 °C. We analysed convex corners with sides along the <n10> crystallographic directions in the masking layer where $1 < n < 8$. These convex corners were stable during etching. As there the compensation that typically leaves residues is not required, our findings allow fabrication of good quality Y-bifurcated microchannels for microfluidics [29–31]. In Ref.[32], the authors fabricated bifurcated silicon channels in the <100> and <110> directions using TMAH-Triton etchant to reduce convex corner underetching. In addition to all the etched silicon microstructures without any compensation using 25 wt % TMAH+NC-200, authors in Ref.[22] presented a Y-bifurcated microchannel. We demonstrate basic designs with sides along predetermined <n10> crystallographic directions different from the standard <110> direction etched in pure 25 wt % TMAH water solution. The presented convex corners provide possibilities for various novel designs with angles that are deflected from the standard <100> direction. The combination of presented basic patterns allows the production of complex silicon microfluidic platforms, especially networks of microchannels [33].
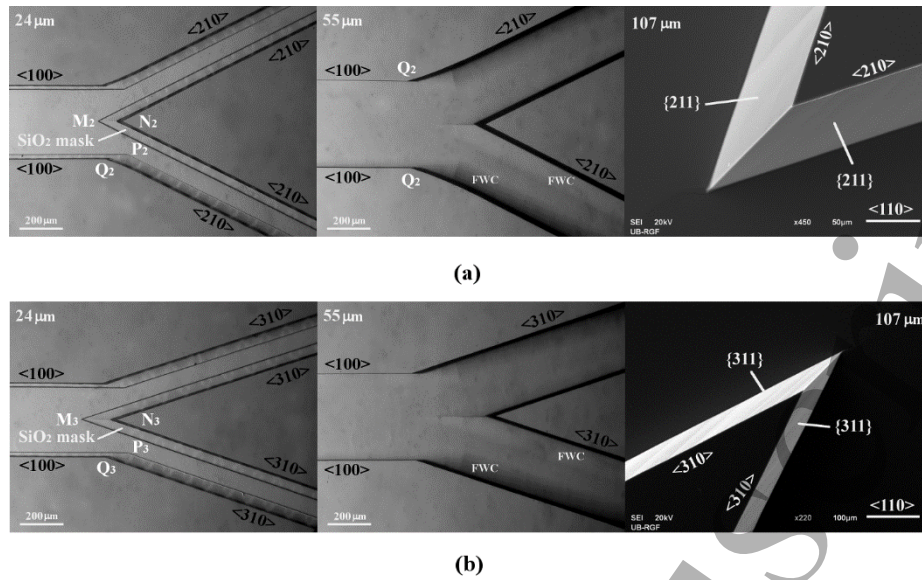
Figure 2. Photographs and SEM microphotographs of etching evolution of Y-bifurcated microchannels with the sides along crystallographic directions <100> and: a) <210>, b) <310>. The SiO_2 masking layer is present in the photographs for the etch depth of 24 μm. SiO_2 is removed after reaching etch depths of 55 and 107 μm. The SEM microphotographs present enlarged convex corners etched from acute angles in the masking layer.

2. Experimental setup

In our experiments [15–16,26–28], we used phosphorus-doped {100} - oriented 3" silicon wafers (SWI) with double-sided polished surfaces. The resistivity of the wafers was 1-5 Ω.cm. The wafers were cleaned in a standard procedure using a freshly prepared mixture of concentrated sulfuric acid and hydrogen peroxide, followed by RCA processing steps (mixture of ammonium hydroxide, hydrogen peroxide, and water; mixture of hydrochloric acid, hydrogen peroxide, and water). Wet thermal oxidation was performed at 1100 ℃ to obtain a SiO_2 masking layer. We defined bifurcations with sides along the predetermined crystallographic directions in the photolithographic processes using buffered hydrofluoric acid (BHF). After photolithographic processes, the wafers were again cleaned using the standard procedure. Native SiO_2 was removed as the wafers were dipped for 30 s in hydrofluoric acid HF (10%) and then rinsed in deionised water. Anisotropic etching was performed in pure TMAH 25 wt. % water solution (Merck) at the temperature of 80 ℃.

Wafers were etched in a thermostated glass vessel closed with a Teflon lid. The vessel was on the top of a hot plate where the TMAH solution temperature was stabilised within ±0.5 ℃ by the electronic temperature controller. The evaporation during etching was minimised using a Teflon lid that included a water-cooled condenser. The glass vessel contained approximately 0.8 dm^3 of the solution. The velocity of the electromagnetically stirred TMAH solution was 300 rpm. We oriented the wafers vertically in a Teflon basket during etching. At the end of the silicon etching, the masking layer was removed using the BHF.

3. Results and discussion

Bifurcated microchannels are designed with sides along the predetermined crystallographic directions <n10> (1 < n < 8) and <100>, as shown in Figures 1-4. Bifurcations consist of two obtuse and one acute angle in the masking layer, with the values mentioned in Table 1. The obtuse angles in the masking layer (angle P in Figure 1(a), angles P_n, n>1 in Figures 2-4) were formed by the <n10> and <100> crystallographic directions, as in Ref.[28]. In the first case of n=2, the sidewalls are defined by {211}–{311} families along the initial <210> crystallographic direction (Figure 2a), as in the case of an etched square with sides along the <210> crystallographic directions presented in Ref.[26,28]. The transition from {211} to {311} planes is smooth. In addition, a smooth distortion of the obtuse angle Q_2 is observed because it is defined by the {100} and {311} planes. The sidewalls of the etched obtuse angle in all other cases (n>2) are defined only by the {n11} and {100} families, as shown in Figures 2(b),3,4. The sidewalls aligned with the <n10> direction belong to the {n11} crystallographic planes, as in Ref.[28]. The angles γ_{n11} between the {n11} and {100} planes are given in Table 2. In the cases where n>2, the sidewalls developed at the obtuse angles Q_n sustain as the etching continues [28].

The acute angles (angle M in Figure 1(a)) of the presented bifurcations are formed in symmetrical <n10> crystallographic directions with respect to the predetermined <100> crystallographic direction. Angles α_{n10} between the appropriate <n10> and <100> crystallographic directions are smaller than 45 °. The acute angles in the masking layer are represented by $2\alpha_{n10}$, which are provided in Table 1. The sidewalls of acute angles aligned to the <n10> directions are from the {n11} families [26,28]. We also analysed two acute angles formed by the <n10> and <m10> crystallographic directions, where m≠n, as shown in Figure 5. The sidewalls of these asymmetrical acute angles in Figure 5 are defined by the {311} and {411} families as well as by the {311} and {511} families. These acute angles can be used for the fabrication of bifurcations with asymmetrical microchannels. In addition, the 3D silicon shape obtained in Figure 5 can

(a)

(b)

Figure 3. Photographs and SEM microphotographs of etching evolution of Y-bifurcated microchannels with sides along crystallographic directions <100> and: a) <410>, b) <510>. The SiO₂ masking layer is present in the photographs for the etch depth of 24 µm. SiO₂ is removed after reaching etch depths of 55 and 107 µm. The SEM microphotographs present enlarged convex corners etched from acute angles in the masking layer.

(a)

(b)

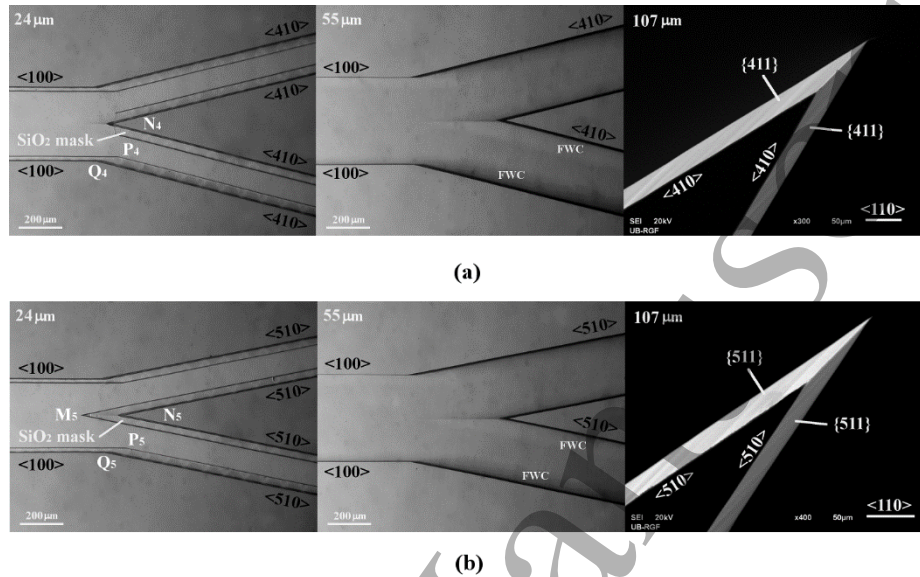Figure 4. Photographs and SEM microphotographs of etching evolution of Y-bifurcated microchannels with sides along crystallographic directions <100> and: a) <610>, b) <710>. The SiO₂ masking layer is present in the photographs for the etch depth of 24 µm. SiO₂ is removed after reaching etch depths of 55 and 107 µm. The SEM microphotographs present enlarged convex corners etched from acute angles in the masking layer.
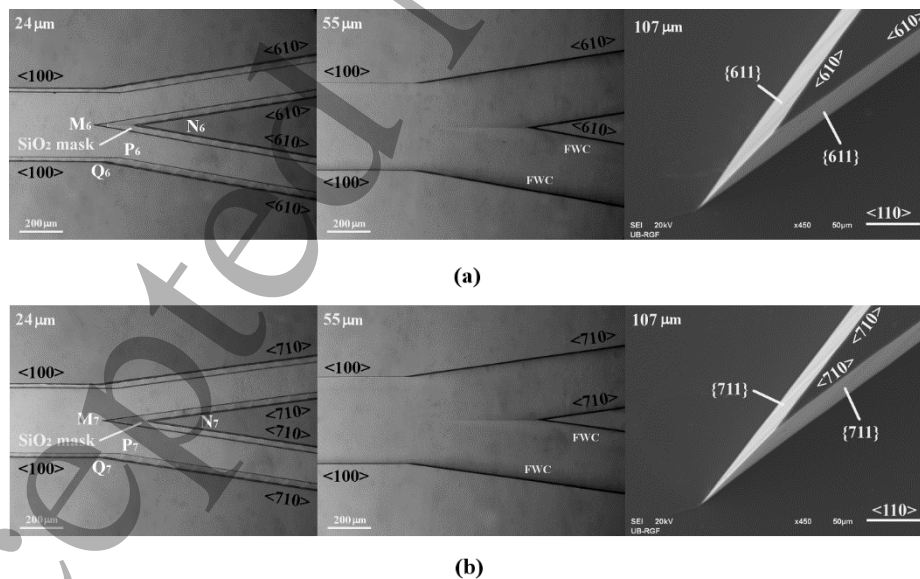
be used as an integrated obstacle in microchannels on the platforms that are based on obstacle mechanisms such as micromixers [28]. As no new crystallographic planes appear during etching, none of the observed acute angles is distorted

Fluid flow in fabricated microchannels can be affected by the residues caused by the convex corner compensation. As no convex corner compensation is applied, there are no residues at the bottom of the etched silicon microchannels. There are facets with a weak curvature (FWC) [15] at every connection of the sidewalls with the bottom surface. The appearance of FWC is inevitable and cannot be compensated in any way. The angles of these facets cannot be determined because of the smooth transition from the bottom to the sidewalls. The appearance of the smooth FWC can influence the cross-sectional shapes of the obtained microchannels.

The widths of the etched microchannels $w_{100etched}$ and $w_{n10etched}$, as presented in Figure 1(a), depend on the etch depth d_{100}:

$$w_{100etched} = w_{100} + 2d_{100} \tag{1}$$

$$w_{n10etched} = w_{n10} + 2\frac{r_{n11}}{r_{100}sin\gamma_{n11}}d_{100} = w_{n10} + 2U_{n11}d_{100} \tag{2}$$

$$U_{n11} = \frac{r_{n11}}{r_{100}sin\gamma_{n11}} \tag{3}$$

where w_{100} and w_{n10} are the widths of the microchannel with sides along the <100> and <n10> crystallographic directions,

respectively, before etching, r_{n11} is etch rate of the {n11} crystallographic planes and U_{n11} is the undercut ratio defined only along one <n10> side of the parallelogram [28]. In Table 2, we provide the values of r_{n11}, γ_{n11}, and U_{n11} [26,28]. The value of {100} etch rate r_{100} is 0.46 µm/min [26]. As an example, we also present in Table 2 widths $w_{n10etched}$ that are calculated using formula (2) and measured in experiments for etch depth of 55 µm.

The vertices of the acute and obtuse angles in the masking layer change their position during etching, as indicated by P→Q and M→N in Figure 1. The position of the vertices depends on the values of r_{n11} and r_{100}, and should be considered during the design of bifurcations:

$$d_{n1o} = U_{n11}d_{100} \tag{4}$$

$$X_{P \to Q} = \frac{d_{n10}}{sin\alpha_{n10}} - \frac{d_{100}}{tg\alpha_{n10}} = d_{100}\left(\frac{U_{n11}}{sin\alpha_{n10}} - \frac{1}{tg\alpha_{n10}}\right) \tag{5}$$

$$Y_{P \to Q} = d_{100} \tag{6}$$

$$X_{M \to N} = \frac{d_{n10}}{sin\alpha_{n10}} = d_{100}\frac{U_{n11}}{sin\alpha_{n10}} \tag{7}$$

where, $X_{P \to Q}$, $Y_{P \to Q}$ and $X_{M \to N}$ are the absolute displacements of vertices in the x and y directions (<100> crystallographic directions). The derived analytical relation allows good control over the dimensions during the etching of the silicon structure in anisotropic TMAH 25 wt. % water solution.

Table 1. Acute and obtuse angles of microchannels.

Crystallographic direction <n10>	Angle between <n10>and<100> α_{n10}[˚]	Acute angle $2\alpha_{n10}$[˚]	Obtuse angle [˚]
<210>	26.6	53.2	153.4
<310>	18.4	36.8	161.6
<410>	14	28	166
<510>	11.3	22.6	168.7
<610>	9.5	19	170.5
<710>	8.1	16.2	171.9

Table 2. Angles γ_{n11} between planes {n11} and {100}, etch rates r_{n11}, ratios of undercut and etch depth U_{n11}, predetermined widths w_{n10}, calculated $w_{n10etched\_c}$ and measured $w_{n10etched\_m}$ widths for etched depth of 55 µm.

Crystallograhic plane {n11}	Angle $\gamma_{n11theoretical}$ [˚]	Angle γ_{n11} [26] [˚]	Etch rates r_{n11} [26] [µm/min]	U_{n11} [28]	w_{n10} [µm]	$w_{n10etched\_c}$ [µm]	$w_{n10etched\_m}$ [µm]
{211}	65.9	66.7	0.87	2.06	70	297	306
{311}	72.5	74.2	0.93	2.10	70	301	307
{411}	76.4	78.7	0.85	1.89	90	298	299
{511}	78.9	80.9	0.81	1.78	100	296	288
{611}	80.7	81	0.73	1.61	120	297	288
{711}	82	83.1	0.69	1.52	130	297	286

In our previous work [26], we analysed the etching of square apertures with sides along the <n10> crystallographic directions. In cases where n>1, the initial right concave corners changed into three new concave corners during etching. One of the angles is formed by the <n10> and <100>

crystallographic directions (angle R in Figure 1(a)), and the value of the concave angle in the masking layer is $180°+\alpha_{n10}$. The sidewalls of the concave angle are also defined by planes of {n11} and {100} families, in the same way as the etched obtuse angle of bifurcation explained above.

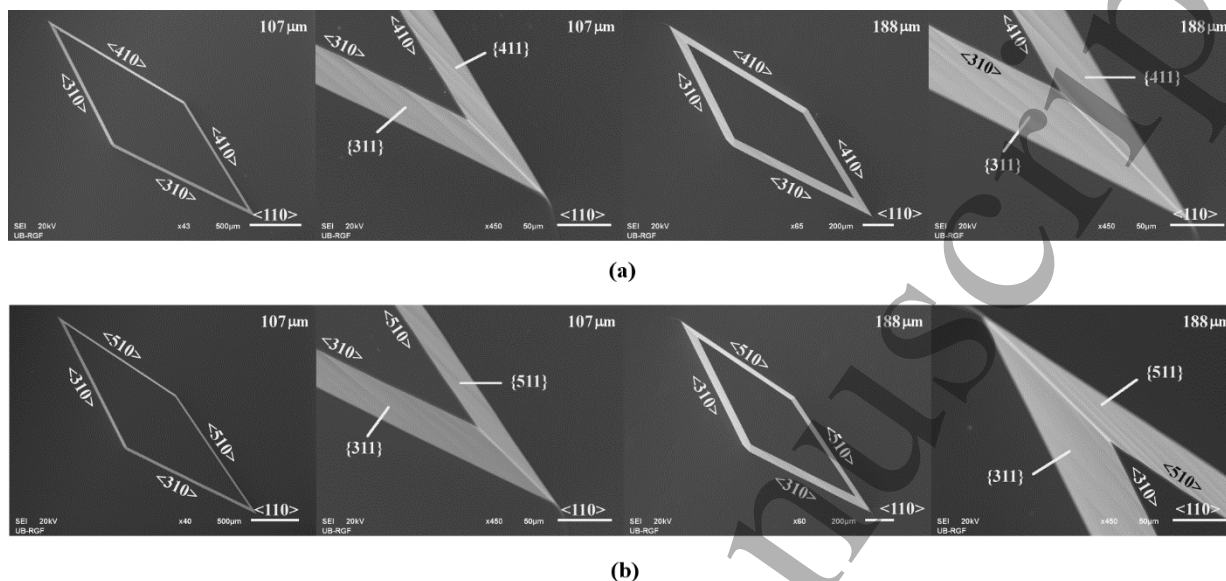Figure 5. SEM microphotographs of etching evolution of 3D silicon structure with sides in the masking layer along crystallographic directions: a) <310> and <410>, b) <310> and <510>. Enlarged convex corners etched from asymmetrical acute angles in the masking layer are given. SiO_2 is removed after reaching etch depths of 107 and 188 µm.
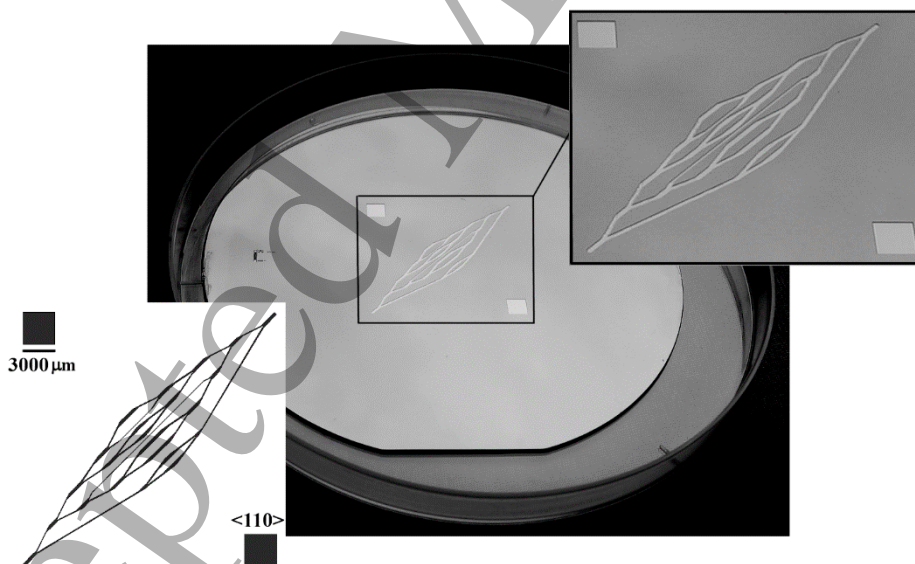
Figure 6. Mask pattern and photograph of multilevel microfluidic network of etched microchannels. The etch depth is 55 µm.

Etching of various convex corners without compensation presented in this study, together with undistorted convex and concave angles from our previous work [26,28] enables the fabrication of multilevel microfluidic networks, as shown in

Figure 1(b),6. Figure 6 shows etched bifurcations with different angles and widths of microchannels that present an example of a complex microfluidic network. The combination of microchannels with sides along <n10> and <100>

crystallographic directions has a significant practical impact because of its simple design and fabrication. In addition, wet etching of silicon in 25 wt % TMAH water solution is a cost-effective process in comparison with dry etching commonly used for various microfluidic platforms [34–37]. The double-sided polished wafer enables double-sided etching to form microchannels on the top side. It also provides inlets and outlets for fluid flow at the bottom side. In this case, micromachining of Pyrex glass is not necessary. The double-side etched wafers anodically bonded to Pyrex glasses on the silicon top sides are more rigid microfluidic platforms than those obtained from polydimethylsiloxane (PDMS) [38–39]. The anodic bonding of Pyrex glass and silicon wafers provides good sealing. In addition, there is no gas permeability as in the case of the most common platforms based on PDMS [40]. Predictable evolution of explored convex and concave corners in this study can be used in future fabrication of other silicon microdevices and platforms. The proposed technique allows the fabrication of predetermined convex corners for microfluidic applications. However, it cannot provide a method to fabricate circular or other irregular geometries of the microchannels.

4. Conclusion

In this technical note, the silicon etching of Y-bifurcated microchannels using 25 wt % TMAH water solution at the temperature of 80 °C has been explored. The sides of the microchannels were designed along the <n10> and <100> crystallographic directions. We demonstrated basic designs of bifurcations with sides along crystallographic directions that are different from the commonly used <110> direction. We obtained convex corners of silicon microfluidic structures that are not distorted during etching, and consequently, no convex corner compensation was applied. The sidewalls of the microchannels are defined by etched planes of the {n11} and {100} families. Analytical relations for the position of angle vertices are determined in order to obtain controllable shapes of microchannels. The presented simple mask designs can be used to fabricate complex microfluidic networks by a cost-effective process with good control over microchannel dimensions.

Acknowledgements

References

[1] Gosalvez MA, Zubel I and Viinikka E 2010 Wet Etching of Silicon in *Handbook of Silicon Based MEMS Materials and Technologies*, Lindroos V, Tilli M, Lehto A, Motooka T (William Andrew, Elsevier). https://www.elsevier.com/books/handbook-of-silicon-based-mems-materials-and-technologies/tilli/978-0-8155-1594-4

[2] Frühauf J 2005 *Shape and Functional Elements of the Bulk Silicon Microtechnique*(Springer-Verlag, Berlin). http://www.springer.com/gp/book/9783540221098

[3] Pal P and Sato K 2017 *Silicon wet etching for MEMS* (Taylor&Francis, Pan Stanford Publishing, Singapore)

[4] Shikida M, Sato K, Tokoro, K and Uchikawa D 2000 Differences in anisotropic etching properties of KOH and TMAH solutions *Sensors and Actuators A* 80 179-188. https://doi.org/10.1016/S0924-4247(99)00264-2

[5] Sato K, Shikida M, Yamashiro T, Asaumi K, Iriye Y and Yamamoto M 1999 Anisotropic etching rates of single-crystal silicon for TMAH water solution as a function of crystallographic orientation *Sensors and Actuators A* 73 131-137. https://doi.org/10.1016/S0924-4247(98)00271-4

[6] Resnik D, Vrtacnik D, Aljancic U and Amon S 2000 Wet etching of silicon structures bounded by (311) sidewalls *Microelectronic Engineering* 51-52555-566. https://doi.org/10.1016/S0167-9317(99)00519-5

[7] Resnik D, Vrtacnik D and Amon S 2000 Morphological study of {311} crystal planes anisotropically etched in (100) silicon: role of etchants and etching parameters *J. Micromech. Microeng.* 10 430-439. https://doi.org/10.1088/0960-1317/10/3/319

[8] Yang H, Bao M, Shen S, Li X, Zhang D and Wu G 2000 A novel technique for measuring etch rate distribution of Si *Sensors and Actuators A* 79 136-140. https://doi.org/10.1016/S0924-4247(99)00270-8

[9] Landsberger L M, Naseh S, Kahrizi M and Paranjape M 1996 On Hillocks Generated During Anisotropic Etching of Si in TMAH *IEEE J. Microelectromech. Syst.* 5 2 106-116. DOI: 10.1109/84.506198

[10] Zubel I, Barycka I, Kotowska K and Kramkowska M 2001 Silicon anisotropic etching in alkaline solution IV: The effect of organic and inorganic agents on silicon anisotropic etching process*Sensors and Actuators A* 87 163-171. https://doi.org/10.1016/S0924-4247(00)00481-7

[11] Zubel I 2019 Anisotropic etching of Si *J. Micromech. Microeng.* 29 093002. https://doi.org/10.1088/1361-6439/ab2b8d

[12] Shen J, Chen Y, Zhang F, Zhang D and Gan Y 2019 Morphological and crystallographic evolution of patterned silicon substrate etched in TMAH solutions *Applied Surface Science* 496 143720.

[13] Sarro PM, Brida D, Vlist W vd and Brida S 2000 Effect of surfactant on surface quality of silicon microstructures etched in saturated TMAHW solutions *Sensors and Actuators A* 85 340-345. https://www.sciencedirect.com/science/article/pii/S0924424700003174

[14] Trieu H K and Mokwa W 1998 A generalized model describing corner undercutting by the experimental analysis of TMAH/IPA *J. Micromech. Microeng.* 8 80-83. https://doi.org/10.1088/0960-1317/8/2/009

[15] Smiljanić M M, Jović V and Lazić Ž 2012 Maskless convex corner compensation technique on a (1 0 0) silicon substrate in a 25 wt. % TMAH water solution *J. Micromech. Microeng.* 22 115011. https://doi.org/10.1088/0960-1317/22/11/115011

[16] Smiljanić M M, Radjenović B, Radmilović-Radjenović M, Lazić Ž and Jović V 2014 Simulation and experimental study of maskless convex corner compensation in TMAH water solutio *J. Micromech. Microeng.* 24115003. https://doi.org/10.1088/0960-1317/24/11/115003

[17] Mukhiya R, Bagolini A, Margesin B, Zen M and Kal S 2006<100> bar corner compensation for CMOS compatible anisotropic TMAH etching *J. Micromech. Microeng.* 16 2458-2462. https://doi.org/10.1088/0960-1317/16/11/029

[18] Bagolini A, Faes A and Decarli M 2010 Influence of Etching Potential on Convex Corner Anisotropic Etching in TMAH Solution *IEEE J. Microelectromech. Syst.* 19 5 1254-1259. DOI: 10.1109/JMEMS.2010.2067436

[19] Mukhiya R, Bagolini A, Bhattacharyya TK, Lorenzelli L and Zen M 2011 Experimental study and analysis of corner compensation structures for CMOS compatible bulk micromachining using 25 wt% TMAH *Microelectronics Journal* 42 127-134. https://doi.org/10.1016/j.mejo.2010.08.018

[20] Merlos A, Acero M C, Bao M H, Bausells J and Esteve J 1992 A study of the undercutting characteristics in the TMAH-IPA system *J. Micromech. Microeng.* 2 181-183. https://doi.org/10.1088/0960-1317/2/3/014

[21] Merlos A, Acero M C, Bao M H, Bausells J and Esteve J 1993. TMAH/IPA anisotropic etching characteristics *Sensors and Actuators A* 37-38 737-743 . https://doi.org/10.1016/0924-4247(93)80125-Z

[22] Pal P, Sato K, Shikida M and Gosalvez M A 2009 Study of corner compensating structures and fabrication of various shape of MEMS structures in pure and surfactant added TMAH *Sensors and Actuators A* 154192-203. https://doi.org/10.1016/j.sna.2008.09.002

[23] Pal P, Sato K and Chandra S 2007 Fabrication techniques of convex corners in a (100)-silicon wafer using bulk micromachining: a review *J. Micromech. Microeng.* 17 R111-R133. https://doi.org/10.1088/0960-1317/17/10/R01

[24] Powell O and Harrison H B 2001 Anisotropic etching of {100} and {110} planes in (100) silicon *J Micromech. Microeng* 11 217-220. http://iopscience.iop.org/article/10.1088/0960-1317/11/3/309

[25] Pal P, Sato K, Gosalvez M A and Shikida M 2007 Study of rounded concave and sharp edge convex corners undercutting in CMOS compatible anisotropic etchants *J. Micromech. Microeng.* 17 2299–2307. https://doi.org/10.1088/0960-1317/17/11/017

[26] Smiljanić M M, Radjenović B, Radmilović-Radjenović M, Lazić Ž and Jović V 2019 Evolution of Si crystallographic planes-etching of square and circle patterns in 25 wt % TMAH *Micromachines*10(2) 102.https://doi.org/10.3390/mi10020102

[27] Smiljanić M M, Lazić Ž, Radjenović B, Radmilović-Radjenović M, Jović V, Rašljić M, Cvetanović Zobenica K and Filipović A 2019 Etched Parallelogram Patterns with Sides Along <100> and <n10> Directions in 25 wt % TMAH *Proc. 6th Conf. IcETRAN, Srebrno jezero, Serbia, Jun. 3–6.*

[28] Smiljanić M M, Lazić Ž, Jović V, Radjenović B and Radmilović-Radjenović M 2020 Etching of Uncompensated Convex Corners with Sides along <n10> and <100> in 25 wt% TMAH at 80 °C *Micromachines* 11(3), 253. https://doi.org/10.3390/mi11030253

[29] Chen P C, Wang Y N and Wu M H 2015 Development of bifurcation microchannel to uniformly distribute a liquid plug, *Chemical Engineering Research and Design* 102 253–260.https://doi.org/10.1016/j.cherd.2015.06.034

[30] Yang J, Pak Y E and Lee T R 2016 Predicting bifurcation angle effect on blood flow in the microvasculature *Microvascular Research* 108 22-28. DOI: 10.1016/j.mvr.2016.07.001

[31] Hymel S J, Lan H, Fujioka H and Khismatullin D B 2019 Cell trapping in Y-junction microchannels: A numerical study of the bifurcation angle effect in inertial microfluidics *Phys. Fluids* 31 082003.https://doi.org/10.1063/1.5113516

[32] Resnik D, Vrtačnik D, Aljančić U, Možek M, Penić S and Amon S 2007 Improvements of Roughness Control in Micromachining of Silicon Microchannels *Proceedings of 5th International Conference on Nanochannels, Microchannels, and Minichannels, June 18–20, Puebla, Mexico ICNMM2007-30217* 133-140. https://doi.org/10.1115/ICNMM2007-30217

[33] Olanrewaju A, Beaugrand M, Yafia M and Juncker D 2018 Capillary microfluidics in microchannels: from microfluidic networks to capillaric circuits *Lab on a Chip* 18 2323. DOI: 10.1039/c8lc00458g

[34] Zhang L, Jones B, Majeed B, Nishiyama Y, Okumura Y and Stakenborg T2018 Study on stair-step liquid triggered capillary valve for microfluidic systems *J. Micromech. Microeng.* 28 065005. https://doi.org/10.1088/1361-6439/aab40c

[35] Agah M, Potkay J A, Lambertus G, Sacks R and Wise K D 2005 High-Performance Temperature-Programmed Microfabricated Gas Chromatography Column *J. Microelectromech. Syst.* 14 1039-1050.**DOI: 10.1109/JMEMS.2005.856648**

[36] Cho Y H, Yamamoto T, Sakai Y, Fujii T and Kim B 2006 Development of Microfluidic Device for Electrical/Physical Characterization of Single Cell*J. Microelectromech. Syst.* 15 1039-1050.DOI: 10.1109/JMEMS.2005.863738

[37] Mihailović M, Rops C M,Hao J, Mele L, Creemer J F and Sarro P M 2011 MEMS silicon-based micro-evaporator *J. Micromech. Microeng.* 21 075007. https://doi.org/10.1088/0960-1317/21/7/075007

[38] Roh C, Lee J andKang C K 2016 Physical Properties of PDMS (Polydimethylsiloxane) Microfluidic Devices on Fluid Behaviors: Various Diameters and Shapes of Periodically-Embedded Microstructures *Materials* 9 836. DOI: 10.3390/ma9100836

[39] Kang C K, Roh C and Overfelt R A 2013 Pressure-driven deformation with soft polydimethylsiloxane (PDMS) by a regular syringe pump: challenge to the classical fluid dynamics by comparison of experimental and theoretical results *RSC Advances* 4 3102-3112. DOI: 10.1039/C3RA46708B

[40] Merkel T C, Bondar V I, Nagai K, Freeman B D and Pinnau I 2000 Gas sorption, diffusion, and permeation in poly(dimethylsiloxane) *Polymer Physics* 38 415-434 https://doi.org/10.1002/(SICI)1099-0488(20000201)38:3<415::AID-POLB8>3.0.CO;2-Z